A High-Dynamic-Range-Based Approach for the Display of Hyperspectral Images

Sarp Ertürk, *Member, IEEE*, Seçil Süer, and Hatice Koç

***Abstract*—This letter presents a new approach for hyperspectral image visualization based on high-dynamic-range (HDR) image processing. The proposed approach is inspired by techniques that are used to display HDR images on low-dynamic-range media by reducing the contrast, yet preserving the image detail. This is the first time this concept is utilized for the display of hyperspectral images. In the presented approach, an edge-preserving filter, called the bilateral filter, is used to extract the base and detail images, and the final image is reconstructed by reducing contrast in the base image but preserving the detail, so that the significance of the detail image is enhanced. It is shown that the proposed approach improves the visual appearance and perceived detail of hyperspectral images.**

***Index Terms*—Bilateral filter, high dynamic range (HDR), hyperspectral imaging, visualization.**

I. Introduction

HYPERSPECTRAL imaging systems acquire visual data in hundreds of spectral bands, resulting in a multidimensional image with a large amount of spectral information. The high spectral resolution provides an increased capability for many image processing tasks with respect to standard imaging systems [1]. However, visualization of the high-dimensional data on traditional display devices, for practical applications, requires dimensionality reduction. Typically, the high number of image bands should be reduced to at most three channels so that it becomes possible to map the components to the widely used red–green–blue (RGB) color space. It is important to obtain three appropriate channels that preserve visual information and enable interpretability [2].

Linear projection methods, such as independent component analysis [3] and principal component analysis [4], have been presented in the literature to obtain the first three principal bands that are assigned as R, G, and B channels. However, in addition to relatively high computational complexity, these approaches do not ensure that the constructed bands are ranked according to image content. Improved linear spectral combination methods such as noise-adjusted principal component analysis [5], interference and noise-adjusted principal component analysis [5], and color matching function [6] have been also presented in the literature. In [7], it has been proposed to fuse spectral bands using the weight obtained through bilateral filtering, so that the weight of each band will be determined according to the amount of detail included in that band.

Band selection approaches have been proposed in the literature to find suitable bands directly from the hyperspectral data. One-bit transform [8], normalized information [9], mutual information [10], spectral information divergence [11], as well as minimum estimated abundance covariance and linear prediction [12] are several approaches that can be used for this purpose.

Multiresolution methods based, for instance, on pyramidal decompositions [13], wavelet transforms [14], and Markov random fields [15] have been also reported for the fusion of hyperspectral image bands for display purposes.

This letter presents a new approach for hyperspectral image visualization inspired by high-dynamic-range (HDR) image processing techniques. The proposed approach is based on the bilateral-filtering-based HDR image display procedure presented in [16].

II. Methodology

A. Bilateral Filtering

Bilateral filtering, which was originally presented in [17], is a nonlinear filter that obtains the output as a weighted sum of the input. The weights are determined according to the spatial distance and the intensity difference of neighborhood pixels. The output of the bilateral filter for a pixel x can be formulated as

$$J(x) = \frac{1}{k(x)} \sum_{\xi} f(x,\xi) g\left(I(\xi) - I(x)\right) I(\xi) \qquad (1)$$

where ξ denotes the pixel within the region of support (filtering neighborhood), f is a Gaussian operating in the spatial domain, and g is a Gaussian operating in the intensity domain. The Gaussian f ensures that pixels close in spatial distance get higher weights, whereas pixels farther away get lower weights. The Gaussian g ensures that pixels close in value (intensity distance) get higher weights, whereas pixels with large value differences get lower weights. Here, $k(x)$ is a normalization factor that is equal to the sum of all weights and can be formulated as

$$k(x) = \sum_{\xi} f(x,\xi) g\left(I(\xi) - I(x)\right). \qquad (2)$$

The bilateral filter operates as an edge-preserving smoothing filter. The operation of the bilateral filter is demonstrated in Fig. 1.

Manuscript received January 1, 2014; revised February 10, 2014; accepted March 13, 2014.

The authors are with the Kocaeli University Laboratory of Image and Signal Processing (KULIS), Electronics and Telecommunications Engineering Department, Kocaeli University, Kocaeli 41300, Turkey (e-mail: sertur@kocaeli.edu.tr).

Color versions of one or more of the figures in this paper are available online at http://ieeexplore.ieee.org.

Digital Object Identifier 10.1109/LGRS.2014.2316165

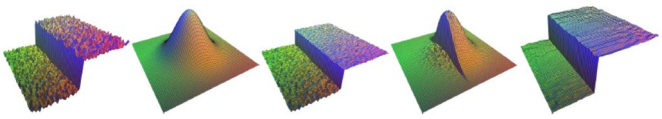

Fig. 1. Bilateral filtering (colors used to convey shape). From left to right: input, spatial kernel f, influence of g for the central pixel, weight $f \times g$ for the central pixel, and output [16].

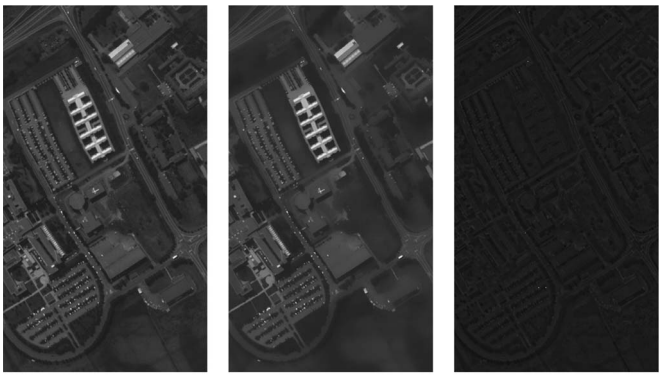

Fig. 2. (a) University of Pavia band #17. (b) Base component. (c) Detail component.

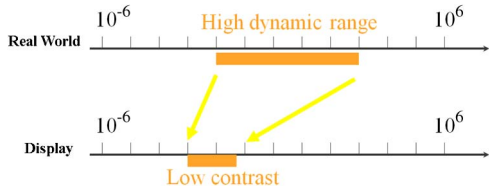

Fig. 3. HDR to low-contrast conversion.

B. Bilateral-Filtering-Based Decomposition

Bilateral filtering is used to decompose an image into a base and a detail component. The base component (also referred to as the large-scale component) is obtained by bilateral filtering of the original image and therefore contains smooth parts and preserved edges. This operation can be denoted by

$$I_{\text{base}} = \text{BF}(I) \tag{3}$$

where BF( ) represents bilateral filtering. The detail component is obtained as the difference between the original image and the base component in the form of

$$I_{\text{detail}} = I - I_{\text{base}} = I - \text{BF}(I). \tag{4}$$

It is seen that the original image is actually equal to the sum of the base component and the detail component. This process is shown for a sample band of the University of Pavia hyperspectral image in Fig. 2.

C. Contrast Reduction Using Bilateral Filtering

As depicted in Fig. 3 for the display of HDR images on conventional equipment, it is necessary to reduce the contrast. If this is directly accomplished on the original image, the image detail is lost as a result of the contrast-reduction process. Therefore, recent approaches separate the original image into a base component (with basically smooth changes, i.e., low spatial frequency) and a detail component (with basically high spatial frequency). The contrast of the base component is reduced, whereas the contrast of the detail component is retained, so that an enhanced contrast reduction is accomplished with preserved detail.

Note that in order to preserve color balance, contrast reduction is performed in the intensity domain for color images [16]. Because contrast is a multiplicative effect, contrast reduction is usually performed in the logarithmic domain [18]. For simplicity, it is possible to use the base-10 logarithm. Therefore, the intensity is first transformed into the logarithmic domain in the form of

$$I_{\log} = \log\ 10(I). \tag{5}$$

Bilateral filtering is applied to the log intensity to extract the base and detail components in the form of

$$I_{\log,\text{base}} = \text{BF}(I_{\log}) \tag{6}$$

$$I_{\log,\text{detail}} = I_{\log} - I_{\log,\text{base}}. \tag{7}$$

Contrast reduction is performed on the base component, and the detail component is retained in the form of

$$I_{\log,\text{new}} = \text{cf} \times I_{\log,\text{base}} + I_{\log,\text{detail}} \tag{8}$$

to provide a low-contrast image with preserved detail. Here, cf denotes the compression factor. Finally, the result is converted from the logarithmic domain back into the linear domain, i.e.,

$$I_{\text{new}} = 10^{I_{\log,\text{new}}}. \tag{9}$$

For color images, this new intensity is combined with the original color channels to obtain the contrast-reduced color image.

III. HDR-Based Display of Hyperspectral Images

Because hyperspectral images have multiple bands that are typically combined for display purposes, it is possible to regard the combined image to be similar to an HDR image in terms of characteristic features. It is therefore proposed in this letter to apply the HDR-based contrast-reduction approach of HDR images to hyperspectral images. For simplicity, and ease of interpretation, three HDR hyperspectral image bands are constructed as the sum of hyperspectral bands falling into the red, green, and blue wavelength ranges. This process can be formulated as

$$\begin{aligned} R_{\text{HDR}} &= \sum_{t \in R} \text{HSI}(t) \\ G_{\text{HDR}} &= \sum_{t \in G} \text{HSI}(t) \\ B_{\text{HDR}} &= \sum_{t \in B} \text{HSI}(t) \end{aligned} \tag{10}$$

where t is used as the band index of the hyperspectral image HSI( ), and R_{HDR}, G_{HDR}, and B_{HDR} are the HDR color

(a) (b)

Fig. 4. University of Pavia image. (a) Original image. (b) Proposed approach.

channels constructed for the hyperspectral image as the sum of bands falling within the corresponding wavelength range.

For simplicity, the intensity channel is computed as the average of color channels in the form of

$$I_{\mathrm{HDR}} = (R_{\mathrm{HDR}} + G_{\mathrm{HDR}} + B_{\mathrm{HDR}})/3. \tag{11}$$

The HDR intensity channel is used to obtain the new intensity channel with reduced contrast and preserved detail, as explained in Section II, which is denoted by I_{LDR}. The new intensity channel is then combined with the color components to obtain the final reduced contrast hyperspectral image to be used for display. For this purpose, it is possible to obtain a pixelwise ratio factor in the form of

$$\text{ratio} = I_{\mathrm{LDR}}/I_{\mathrm{HDR}}. \tag{12}$$

This ratio factor can be used to obtain the final low-dynamic-range color channels in the form of

$$\begin{aligned} R_{\mathrm{LDR}} &= \text{ratio} \times R_{\mathrm{HDR}} \\ G_{\mathrm{LDR}} &= \text{ratio} \times G_{\mathrm{HDR}} \\ B_{\mathrm{LDR}} &= \text{ratio} \times B_{\mathrm{HDR}}. \end{aligned} \tag{13}$$

Fig. 4 shows the proposed approach for the University of Pavia hyperspectral image. Fig. 4(a) depicts the case if all corresponding bands are simply averaged (i.e., using equal weights) to obtain the color channels, and Fig. 4(b) shows the result of the proposed approach. It is seen that the proposed approach provides visually enhanced appearance and increased perceived detail. The normalized average gradient computed over the reconstructed images is obtained to be 0.1735 for the original image provided in Fig. 4(a) and 0.2194 for the image obtained with the proposed approach provided in Fig. 4(b). These values confirm that the proposed approach retains increased detail in the reconstructed image.

(a) (b)

Fig. 5. Part of the University of Pavia image. (a) Original image. (b) Proposed approach.

(a) (b)

Fig. 6. Pavia Centre image. (a) Original image. (b) Proposed approach.

Fig. 5 shows an enlarged part of the University of Pavia image to demonstrate that the proposed approach improves visual appearance.

Fig. 6. presents results for the Pavia Centre hyperspectral image. In this case, the normalized average gradient computed over the reconstructed images is obtained to be 0.1708 for the original image provided in Fig. 6(a) and 0.2328 for the image obtained with the proposed approach provided in Fig. 6(b). It is similarly observed that the proposed approach provides a superior result in terms of visual appearance and color presentation, which is also confirmed by the quantitative evaluation carried out using the average gradient values.

Note that the University of Pavia and Pavia Centre hyperspectral images are captured using the Reflective Optics System Imaging Spectrometer (ROSIS) sensor that has a spectral range between 430 and 860 nm with a bandwidth of 4.0 nm. In the results presented in Figs. 4–6, only hyperspectral bands that fall into the blue, green, and red wavelengths are considered so that the reconstructed images are close to images that would be acquired using a color camera and, hence, are more suitable for visual interpretation. Because of the properties of the ROSIS sensor, these bands already make up about 80% of the totally available hyperspectral bands.

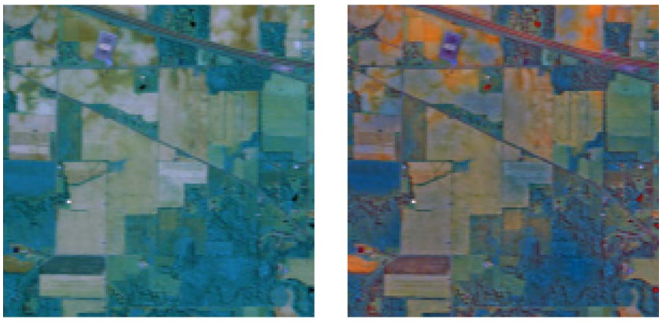

(a) (b)

Fig. 7. Indian Pine image. (a) Original image. (b) Proposed approach.

It is possible to assign the entire range of hyperspectral bands to the three color channels of the reconstructed image using the proposed approach in a straightforward way, if desired, to make use of the full hyperspectral data. Fig. 7 shows results obtained for the Indian Pine data set, in this case, where the total data set includes 220 hyperspectral bands, and these bands are equally divided to be incorporated into the blue, green, and red channels of the color images. The data are captured using the Airborne Visible/Infrared Imaging Spectrometer and has a spectral range between 400 and 2500 nm with a bandwidth of approximately 10 nm. Because all hyperspectral bands are used in the visualization, the reconstructed colors do not correspond to real world colors but are rather pseudocolors. Images provided in Fig. 7 again show that the proposed approach provides improved visual appearance. In this case, the normalized average gradient is 0.2558 for the original image, whereas it is obtained as 0.2768 for the image reconstructed with the proposed approach.

IV. Conclusion

A new method for the visualization of hyperspectral images based on HDR imaging has been presented in this letter. It is shown that the proposed approach can provide improved visual appearance and increased detail perception. In this regard, this letter introduces the concept of HDR-based image processing for the purpose of enhanced visualization to the remote sensing community. It is envisioned that the presented concept can be improved by integrating it into enhanced band extraction/fusion approaches, and it is also possible to investigate the utilization of different HDR-based contrast-reduction approaches.

References

[1] D. A. Landgrebe, *Signal Theory Methods in Multispectral Remote Sensing*. New York, NY, USA: Wiley, 2003.

[2] N. P. Jacobson and M. R. Gupta, "SNR-adaptive linear fusion of hyperspectral images for color display," in *IEEE Int. Conf. Image Process.*, San Antonio, TX, USA, 2007, vol. III, pp. 477–480.

[3] H. Du, H. Qi, X. Wang, and R. Ramanath, "Band selection using independent component analysis for hyperspectral image processing," in *Proc. 32nd Appl. Imagery Pattern Recog. Workshop*, Washington, DC, USA, Oct. 2003, pp. 93–99.

[4] X. Jia and J. A. Richard, "Segmented principal components transformation for efficient hyperspectral remote-sensing image display and classification," *IEEE Trans. Geosci. Remote Sens.*, vol. 37, no. 1, pp. 538–542, Jan. 1999.

[5] Q. Du, N. Raksuntorn, S. Cai, and R. J. Moorhead, "Color display for hyperspectral imagery," *IEEE Trans. Geosci. Remote Sens.*, vol. 46, no. 6, pp. 1858–1866, Jun. 2008.

[6] N. P. Jacobson, M. R. Gupta, and J. B. Code, "Linear fusion of image sets for display," *IEEE Trans. Geosci. Remote Sens.*, vol. 45, no. 10, pp. 3277–3288, Oct. 2007.

[7] K. Kotwal and S. Chaudhuri, "Visualization of hyperspectral images using bilateral filtering," *IEEE Trans. Geosci. Remote Sens.*, vol. 48, no. 5, pp. 2308–2316, May 2010.

[8] B. Demir, A. Celebi, and S. Erturk, "A low-complexity approach for the color display of hyperspectral remote-sensing images using one-bit transform-based band selection," *IEEE Trans. Geosci. Remote Sens.*, vol. 47, pt. 1, no. 1, pp. 97–105, 2009.

[9] S. Le Moan, A. Mansouri, Y. Voisin, and J. Y. Hardeberg, "A constrained band selection method based on information measures for spectral image color visualization," *IEEE Trans. Geosci. Remote Sens.*, vol. 49, no. 12, pp. 5104–5115, Dec. 2011.

[10] B. Guo, S. R. Gunn, R. I. Damper, and J. B. Nelson, "Band selection for hyperspectral image classification using mutual information," *IEEE Geosci. Remote Sens. Lett.*, vol. 3, no. 4, pp. 522–526, Oct. 2006.

[11] C.-I. Chang, "An information-theoretic approach to spectral variability, similarity, discrimination for hyperspectral image analysis," *IEEE Trans. Inf. Theory*, vol. 46, no. 5, pp. 1927–1932, Aug. 2000.

[12] H. Su, Q. Du, and P. Du, "Hyperspectral image visualization using band selection," *IEEE J. Sel. Topics Appl. Earth Obs. Remote Sens.*, to be published.

[13] S. K. Rogers, T. A. Wilson, and M. Kabrisky, "Perceptual-based image fusion for hyperspectral data," *IEEE Trans. Geosci. Remote Sens.*, vol. 35, no. 4, pp. 1007–1017, Jul. 1997.

[14] H. Li, B. Manjunath, and S. Mitra, "Multisensor image fusion using the wavelet transform," *Graph. Models Image Process.*, vol. 57, no. 3, pp. 627–640, May 1995.

[15] M. Mignotte, "A multiresolution Markovian fusion model for the color visualization of hyperspectral images," *IEEE Trans. Geosci. Remote Sens.*, vol. 48, no. 12, pp. 4236–4247, Dec. 2010.

[16] F. Durand and J. Dorsey, "Fast bilateral filtering for the display of high-dynamic-range images," *ACM Trans. Graph.-Proc. ACM SIGGRAPH*, vol. 21, no. 3, pp. 257–266, Jul. 2002.

[17] C. Tomasi and R. Manduchi, "Bilateral filtering for gray and color images," in *Proc. IEEE Int. Conf. Comput. Vis.*, 1998, pp. 836–846.

[18] K. Smith, G. Krawczyk, K. Myszkowski, and H.-P. Seidel, "Beyond tone mapping: enhanced depiction of tone mapped HDR images," *Comput. Graph. Forum*, vol. 25, no. 3, pp. 427–438, 2006.